



Research Article

Sol-gel Derived Sc-doped ZnO:Sc Thin Films: Analysis of Structural, Morphological, Electrical, and Optical Properties Annealed in Different Atmospheres

Ruchika (Sharma) Joshi¹, R. M. Mehra^{2*} and Archana Tripathi¹

¹Department of Physics, Deshbandhu College, University of Delhi, India.

²Ennoble IP Consultancy Pvt. Limited, Noida, Uttar Pradesh, India.

Corresponding author email: rm.mehra@ennobleip.com

ABSTRACT: Transparent conductive oxide (TCO) electrode layers made of high-quality Sc-doped ZnO:Sc (0.0 to 1.5 wt%) thin films have been applied to Corning Glass 7059 substrates for thin film solar cell applications. After growth, annealing treatments lasting an hour were conducted on samples that had been deposited in the same chamber with different ambient atmospheres (air and nitrogen). Through a variety of characterization methods, such as X-ray diffraction (XRD), atomic force microscope (AFM), Hall Effect, and optical absorption measurements, it has been determined how different ambient atmosphere annealing atmospheres affect the electrical, structural, and optical properties of the deposited films. The findings showed that the annealing atmosphere significantly impacted the films' structural, electrical, and optical properties; this effect was more obvious for films annealed in nitrogen ambient. XRD, SEM, and AFM results exhibit the crystallinity and grain size improvement for the films with 0.5 wt % Sc concentration in both the annealing atmosphere (more remarkable in the nitrogen atmosphere). The deterioration of the films was seen with further doping. Both mobility and carrier concentration are higher in the nitrogen atmosphere but the resistivity is lower in the air atmosphere. Under the optimum annealing condition, the lowest resistivity of $2.8 \times 10^{-4} \Omega\text{-cm}$ and highest carrier concentration of $6.4 \times 10^{20} \text{ cm}^{-3}$ has been obtained in these nitrogen-annealed sol-gel derived films with 0.5 wt% Sc concentration. The transmittance of the films shows improvements in nitrogen ambient from 80% to 92% with a wide band gap. RHEED pattern shows the formation of polycrystalline nanorods in the air atmosphere and the growth of single crystals in the nitrogen atmosphere for the films with 0.5 wt % Sc doping. These findings confirmed the stability of the ZnO:Sc films as TCO electrode materials in solar cells and displays.

KEYWORDS: Thin Films, Sol-gel, Sc-doped ZnO:Sc, Nitrogen Ambient, Optical Property.

INTRODUCTION

Zinc oxide is a wurtzite-like hexagonal material semiconductor having constants for the crystalline unit cell $a = 3.24$ and $c = 5.19$, respectively. Four atoms of one type basically surrounds the other type of an atom in tetrahedral fashion such that the two interpenetrated hexagonal lattices seem to be fitted by the position of single atom [1]. Its dominant defects arise due to surplus vacancies at both sites, hence the Zn:O ratio must exceed unity [2]. At 300K it has a broadband gap of 3.3 eV [3]. The exciton is still dominant in the optical process

even at room temperature because it has a significant excitation binding energy of 60 meV [4], making it a strong contender for light-emitting devices such blue LEDs and Lasers [5]. Because of its excellent stability and low toxicity, it is a viable contender to replace indium tin oxide and tin oxide in the production of conductive electrodes for solar cells.

Additionally, it is useful as a phosphor for colour displays, a gas sensor, and thin-film varistors [6]. For the synthesis of ZnO thin films, various thin film deposition techniques are known [14–17]. The sol-gel process method is beneficial for coating manufacturing because it enables simple compositional changes, adaptable microstructures, relatively low annealing temperatures, and the ability to coat on substrates with vast surface areas [18–22] using simple, affordable equilibration techniques. It also provides superb control over the stoichiometry of precursor solutions. Sol-gel constitutions are consequently ideal for preliminary screening-required learning on a variety of materials, compositions, or circumstances. Rare-earth impurities like Scandium (Sc) and Yttrium (Y), whose ionic radius is extremely like that of zinc and makes them suitable with doping, have seldom ever been studied in terms of their effects on performance [23–24]. A drop in grain size brought on by Y doping has been linked to an improvement in hydrogen sensors made from YZO thin films [25].

Despite not belonging to the lanthanide series, the element Sc is sometimes grouped with this group due to its close relationship. Some of its uses include computer screens, fluorescent lighting phosphors, and fuel usage sensors for automobiles. Sc doped ZnO films show that they can be used to create optoelectronic devices [26]. Different atmospheres, such as nitrogen and hydrogen, can change the electrical characteristics of ZnO through thermal treatment. Numerous researchers heated ZnO thin films, such as, Studenikin *et al.* [15] heated these films in nitrogen, Studenikin *et al.* [16] heated these films in hydrogen and oxygen, Rusu *et al.* [1] heated the films in vacuum and oxygen atmosphere, and Studenikin *et al.* [6] heated the films in nitrogen. In this study, 2-methoxy ethanol was taken for solvent and monoethanolamine (MEA) for stabiliser to create Scandium doped (0.0 wt% to 1.5 wt%) ZnO:Sc films using the sol-gel method. These films were then annealed at 400°C in both nitrogen and air ambient environment for 1 hour. Finally, after desired characterizations, it is culminated that Sc doping has a dominant impact on a variety of structural, electrical, optical, and electrical properties. It has also been appraised that ZnO:Sc (0.5 wt%) annealed in a nitrogen environment increases the quality.

Research Highlights

- a. The study reveals that the structural, electrical, and optical properties of Sc-doped ZnO thin films significantly improved by annealing in nitrogen and air.
- b. Nitrogen annealing outperformed air annealing in air.
- c. Nitrogen-annealed films at 0.5 wt% Sc doping demonstrated improved crystallinity, highest carrier concentration ($6.4 \times 10^{20} \text{ cm}^{-3}$), lowest resistivity ($2.8 \times 10^{-4} \Omega \cdot \text{cm}$), and up to 92% transmittance indicating better charge transport properties.
- d. Single-crystal growth was observed in nitrogen, while polycrystalline nanorods formed in air.
- e. The findings highlight the suitability of ZnO:Sc films as transparent conductive electrodes for optoelectronic applications, particularly in solar cells and displays.

EXPERIMENTAL DETAILS

Sample synthesis

By applying Zinc acetate dehydrate $\text{Zn}(\text{CH}_3\text{COO})_2 \cdot 2\text{H}_2\text{O}$ (99.95%, GR, Hayashi Pure Chemical Ind. Ltd, Japan), anhydrous 2-methoxy ethanol (AR, Ajax Chemicals, Australia) and monoethanolamine (MEA, CP, Bio-Lab, London), ZnO:Sc (0.0wt%-1.5wt%) films has been synthesised by the sol-gel route. MEA/Zn solution was stirred for 5 min along with a molar ratio of 0.2. A dopant with a suitable concentration (0.0 to 1.5 wt%) of 99.9% pure $\text{ScNO}_3 \cdot 6\text{H}_2\text{O}$ was added. The mixture was also sonicated for roughly two hours. After 48 hours, the resulting uniform, transparent, and clear solution was applied for film deposition. Microscopic Corning glass (7059) slides used as the substrates were cleaned using ultrasound for 10 minutes each in acetone and methanol. They were then thoroughly cleaned for further 20 minutes in deionized water before being dried in a nitrogen atmosphere. The spinner's spinning speed and spin time were considered as 3200 rpm and 30 s, respectively for film accumulation. The wet films were preserved, dried at 200 °C for the succeeding 10 min, heated at 280 °C for 20 min, and then hydrolyzed in the air for 5 min at ambient temperature with a heating rate of around 10 °C/min. Thus, the drying procedure eliminates the residual organic solvents and organic groups in the deposition sol gel film and transforms the organic precursor film into a concentrated inorganic coating. Each spin will provide an average thickness of 0.02 μm to respective film. To increase the film thickness, the coating and drying steps from above were done innumerable times. The average thickness of the films used in this experiment was between 450 and 500 nm. The deposited films were then annealed for 1 hour in air ambient environment and 1 hour for nitrogen ambient environment, at annealing temperature of 400°C, respectively. To avoid the probability of stress in the films a slow cooling rate was maintained on behalf of rapid cooling.

Characterization

The crystal aspect of Scandium (Sc) doped ZnO:Sc films were investigated with X-ray diffraction (XRD) patterns using Philips PW 1830 Geiger counter diffractometer, PW 1830 to determine the orientation and crystallite phase using a monochromatic X-ray beam with nickel-filtered CuK radiation ($\lambda = 1.5418 \text{ \AA}$). With a 0.02 sample pitch and a 4 deg/min scan rate, slow continuous scan mode was employed to capture 2θ data between 30° and 40°. Scanning electron microscopy (SEM, JEOL JSM-6300) was used for Microstructure investigation. An atomic force microscopy (AFM, Burleigh-SPI 3700) with the scanned area of $5 \times 5 \mu\text{m}^2$ was used to obtain the Average surface roughness of the films. DEKTECK3-ST surface profilometer was used for determining the thickness of the films. Optical transmittance in the region of 300–800 nm, was determined by using a Shimadzu UV-3150 spectrophotometer. The van der Pauw [20] technique was used for measuring the electrical resistivity (ρ). The Hall coefficient R_H and the Hall coefficient's sign confirmed the n-type conduction of the films. The elemental dispersion analysis using X-ray (EDAX) measurements was used to authenticate the composition of scandium-doped ZnO films. The effects of Sc doping (0.0 wt% to 1.5 wt%) were narrated on structural (preferred orientation, surface morphology), electrical (resistivity, carrier concentration, and Hall mobility), and optical (transmittance, band gap) properties. Using the band gap expansion and narrowing phenomena, the fluctuation of the band gap with doping was examined.

RESULTS AND DISCUSSION

Structural properties

By using XRD, SEM, and AFM, the interfacial characteristics of ZnO:Sc (0.0 wt% - 1.5 wt%) films on corning substrate were inspected.

X-ray Diffraction (XRD) investigation:

Powder X-ray diffraction patterns have been investigated to examine the structural characteristics and phase purity. The XRD results of the synthesized ZnO:Sc (0.0 wt% to 1.5 wt%) films annealed in nitrogen and air atmospheres with a heating rate of 2°C/min exhibited.

A specific annealing temperature (400°C) was kept for 10 min for measurement. Figure 1(a-f) depicts the peak intensity, 2θ , FWHM, lattice constant, and grain size D (nm) for ZnO:Sc (0.0 to 1.5 wt%) films annealed at 400°C in air and nitrogen ambient environment for 1h. The powerful and strong peaks in Fig. 1 (a) manifest that all of the samples have a high crystallinity. In all compositions, the analysis of the diffraction peaks showed the presence of the ZnO structural phase known as wurtzite, which is near to the standard diffraction pattern (JCPDS Card No. 80-00075), and no sign of any scandium-related phase, such as metallic scandium, scandium oxides, or any binary zinc scandium phase, was found for the samples that were doped with 0.5, 1.0, and 1.5 weight percents of scandium. This exhibits that the Sc^{+3} ions replaced Zn positions without significantly changing the crystal structure of ZnO. In view of the fact that Sc may easily enter the ZnO crystal lattice as ionic radii of Zn^{+2} and Sc^{+3} being 72 pm and 69 pm, respectively. However, extremely faint peaks corresponding to SnO started to develop around 1.5 wt% Sc doping, and it has been discovered that these peaks intensify as Sc doping percentages rise. So, for 1.5 wt% Sc doping, ScO started segregating.

Therefore, at lower Sc doping concentrations, its ions can effectively replace Zn ions. However, as Sc concentration rises, ScO begins to cluster and is isolated as an impurity phase in both the nitrogen and air annealing atmospheres. In accord with Fig. 1(b), Scandium substitutional doping up to 0.5 wt% brings forth the increase in peak intensity. The peak intensity is expected to depend upon Zn and with the substitutional doping Zn may increase the peak intensity. Fig 1(a, c) illustrates a dominant peak at $2\theta = 34.44^\circ$ conforming to the (002) plane of ZnO and other peaks corresponding to (100) and (101), pointing the polycrystalline nature of the films as evidenced by RHEED pattern. Fig 1(b) shows the variation of intensity for ZnO:Sc (0.0 to 1.5 wt. %) films with maximum intensity at 0.5 wt %. Fig 1(c) shows in ZnO:Sc (0.0 wt%-1.5 wt%) films, 2θ value varies from 34.39° to 34.46° and 34.38° to 34.54° annealed at 400° in air and nitrogen ambient temperature respectively. This implies that Sc replaces Zn in the hexagonal lattice [27]. The film having 1.5 wt% of Sc showed a maximum shift in the (2θ) value. The observed variation in the shift may be due to excess/ heavy Sc doping. Fig. 1(f) foretells that with increasing Sc dopant concentration up to ZnO:Sc (0.5 wt%) the relative intensity of the (002) peak was found to increase, and then it began to decline with an increase in FWHM, indicating the degradation in the crystallinity and reduction in grain size of the film in both atmospheres. Resultant of intrinsic defects such Zn interstitials (Zn_{ni}) and oxygen vacancies that departing from stoichiometry and generate a Zn:O ratio greater than unity, ZnO is naturally an n-type semiconductor [28, 29].

The Debye-Scherrer equation has been used to countermeasure the whole width at the half-maximum of the most intense diffraction peak (1 0 1) in order to ponder the average crystallite size [30].

$$D = 0.9 * \lambda / \beta * \cos(\theta) \dots (1)$$

where D is the average crystallite size, λ is the wavelength of the incident X-ray beam (1.541 Å), β is the angular width of the diffraction peak at the half maximum in radians on 2θ scale and θ is the Bragg's diffraction angle. The dominant crystallite size for ZnO:Sc (0.0 to 1.5 wt%) films is 4.19 nm at 0.5 wt% in air and 4.92 nm annealed at 400° in nitrogen, respectively.

The average particle size and film crystalline size were reduced when Sc dopant concentration increased by more than 0.5 wt%, which has a lower radius than the host atoms. Because of the lattice distortion brought on by the difference in radii between the replacement atom in ZnO and the Sc dopant, crystallite size is therefore reduced. The results are obtained with a 0.5 wt% Sc concentration since the crystalline average size should be achievable at a reasonable pace. The gap between Sc and Zn ionic radius led to crystalline deformation as Sc concentration increased (beyond 1.5 wt%). Up to 0.5 weight percent of Sc dopant concentration, it has been found, crystallite size increases; nevertheless, at greater dopant concentrations, grain size declines. A high number of crystallites are habituated along the c-axis, as authenticated by the increase in crystallite size of the film with Sc concentration of 0.5 wt%.

With an increase in dopant concentration, ZnO:Sc samples lattice constant 'c' values were found to be moderately lower than those of pure ZnO films, as indicated. The measured values fall between 5.195 and 5.215 and between 5.200 and 5.214 when annealed at 400 degrees Celsius for air and nitrogen, respectively. This possibly indicates that the sites available for Scandium in ZnO are limited [31]. The difference in ionic radii between Zn^{+2} and Sc^{+3} is the foundation for shift in the position of the (002) peak as well the change in the lattice constant 'c' value. Additionally, as depicted in Fig. 1(b), the ZnO:Sc films (0 0 2) diffraction peak intensities dropped with higher doping concentrations of greater than 0.5wt%. This strain has the potential to seriously alter as well degrade the development of ZnO crystals. Previous studies have prominent a similar pattern in the loss of crystallinity caused by metal dopants as Eu [32], Ce [33], and Al [34]. The crystal structure of ZnO:Sc (1.5 wt%) that has been annealed in both atmospheres shows degradation. This suggests that an excessive rise in doping concentration degrades the crystallinity of films. This may be because high doping concentrations cause dopants to segregate in grain boundaries and cause stresses to occur because to the difference in ion sizes between zinc and the dopant.

Surface morphology

Scanning electron micrographs (SEM):

Figure 1 surveys the ZnO:Sc (Sc 0.0 to 1.5 wt%) films annealed at 400 °C in an air ambient environment for one hour. Fig. 1(a) speculates that the dendrites nanocrystallites are uniformly dispersed on the surface of films made of pure ZnO:Sc (0.0 wt%) nanomaterials. Three-legged dendrites become nanorod-like structures with a high packing density and granular background that is evenly dispersed across the surface when the scandium concentration in ZnO:Sc materials increases up to 0.5 wt%, as illustrated in Fig. 1(b). The following mechanisms could occur when producing ZnO:Sc from zinc acetate precursor in an oxygen-rich air atmosphere. There are two probabilities of formations of soluble complexes including zinc oxy-acetate and ZnAc-DEA [$Zn(OAc)_2(H_2DEA)$] can happened during sol-gel aging [$Zn_4O(Ac)_6$] [35-36]. These two intermediate complexes may occur before the subsequent breakdown of acetate groups, which starts the synthesis of ZnO:Sc nanorods, during annealing. An oxygen-rich atmosphere can encourage the breakdown and ZnO:Sc formation, increasing the crystallinity of the film annealed in air. Figure 1 (c & d) portray the rapid grain growth with larger grain sizes that could lead to more voids and porosity, under an air ambient atmosphere.

However, in an environment of inert nitrogen, the lack of oxygen may cause a delay in the formation of ZnO:Sc from these intermediate molecules, resulting in the creation of grains but not nanorods in ZnO:Sc firms with Sc concentrations of 0.5 wt% annealed at 400°C. With further increases in scandium concentration (1wt% to 1.5wt%), the crystalline deformation

originates because of the difference between the Sc and Zn ionic radii in the two atmospheres, as also consistent with the XRD results. Nanorod size starts decreasing in the air ambient atmosphere (Fig. 1c, d), and grain size also starts decreasing in the nitrogen ambient atmosphere (Fig. 2c, d).

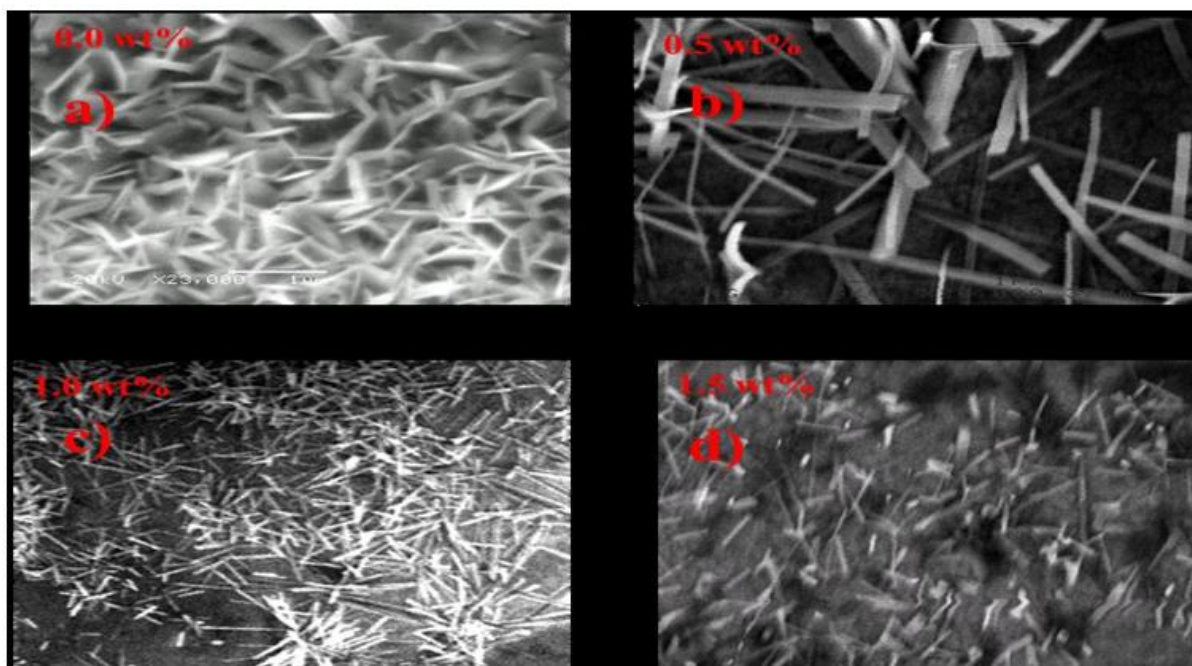


Figure 1: SEM Image of ZnO:Sc (Sc 0.0 to 1.5 wt. %) thin films annealed at 400 °C in air ambient atmosphere for 1 h

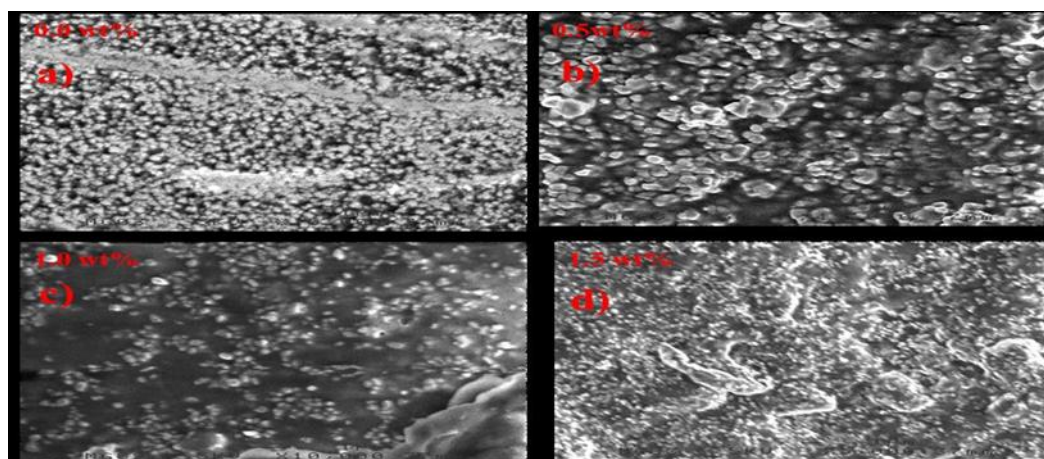


Figure 2: SEM micrographs of ZnO:Sc (Sc 0.0 to 1.5 wt. %) thin films annealed at 400 °C in nitrogen ambient atmosphere for 1 h.

The SEM sculpture of thin ZnO:Sc films (0.0 to 1.5 wt%) annealed at 400 °C in a nitrogen ambient atmosphere for one hour is forecasted in Fig. 3. We can see uniform, spherical granules of a comparable size on the surface of the film in Fig. 3, and we can also see that the size of the granules grows as the Scandium concentration in ZnO:Sc films rises. All of the films had spherical grains, proving that they are polycrystalline and corroborating the XRD findings. Grains between 60 and 100 nm in size can be shown to be closely bonded to one another in Fig. 3(a), and rough sintered surfaces are produced. When the amount of Scandium is raised to

0.5 wt%, as shown in Fig. 3(b), the tiny grains disappear, and grain coalescence and agglomeration lead to the formation of a dominating sediments surface with comprehensible grain boundaries. Even though many apertures smaller than 100 nm in size vanished and striking crystal growth occurred without any voids or cracks, it still has a very low porosity, indicating high-quality films when the grain size exceeds 200 nm. The sintered grains are closely linked to one another and exhibit polyhedral forms. The results of the XRD patterns and the SEM micrographs are consistent, indicating that Sc doping in ZnO:Sc thin films can enhance the average grain size. The enfold grains of the nitrogen ambient atmosphere annealed film have smaller grain sizes and less porosity than samples annealed in an air ambient environment. A comparison of the two films XRD data reveals that the doped film had smaller grains and fewer cavities than the undoped film after being annealed in air. According to morphological research, the amount of dopant affects the morphology and coarseness of the films.

Atomic force microscopy (AFM):

Figure 3 shows AFM images of ZnO in 3D and 2D. Thin films of Zn:Sc (Sc 0.0–1.5 wt%) were annealed for one hour at 400 °C in an environment of ambient air. Images show that as the amount of scandium climbs to 0.5 wt%, the grains' height and size are expanding (Fig. 4(b)). This is due to the process of coalescence, which results in substantial grain expansion. The sample's grains' tips are not particularly sharp, as may be observed. The SEM photos show the exact morphology more clearly than AFM images because nanorods are too sharp for AFM to distinguish them.

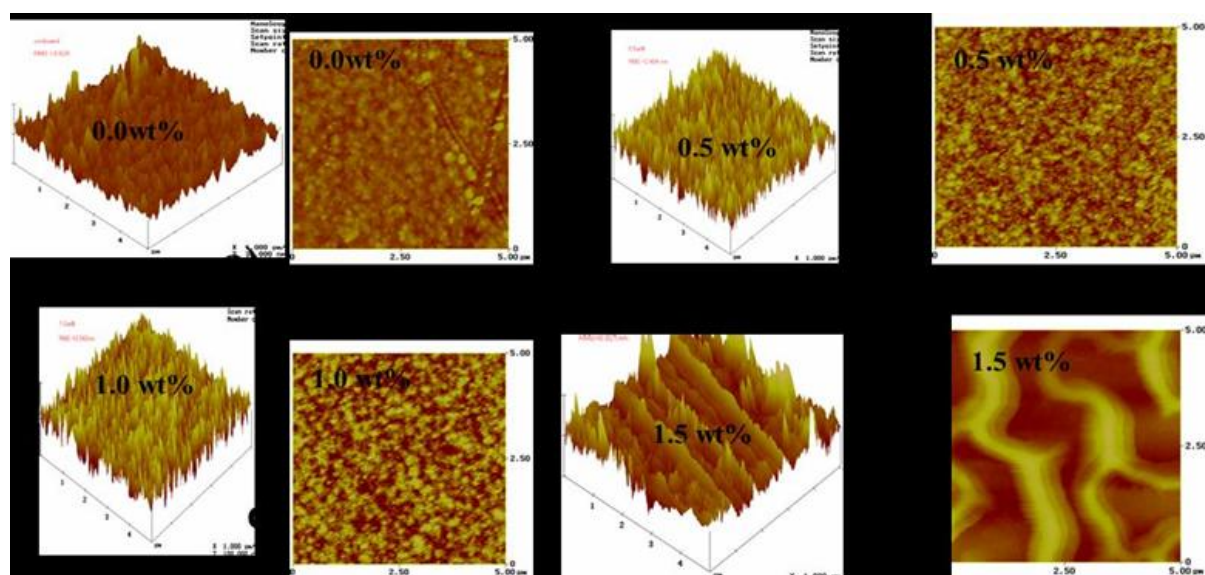


Figure 3: AFM 3D and 2D Images of ZnO:Sc (Sc 0.0 to 1.5 wt. %) thin films annealed at 400 °C in air ambient atmosphere for 1 h.

Surface roughness falls significantly (from 28.8 nm to 4.7 nm) up to 0.5 wt% with an increase in Sc content. Particle sizes in ZnO:Sc (0.0 wt% to 1.5 wt%), films annealed in nitrogen ambient atmosphere were 124 to 160 nm while those in the films annealed under air ambient were 90-100 nm, respectively, analysed in AFM, Fig 5(a to d). AFM and SEM analysis of ZnO:Sc films revealed that the particle size is substantially greater than what XRD had

indicated. This shows that whereas XRD provides the crystallite size, AFM provides the grain size (perhaps a few crystallites linked together).

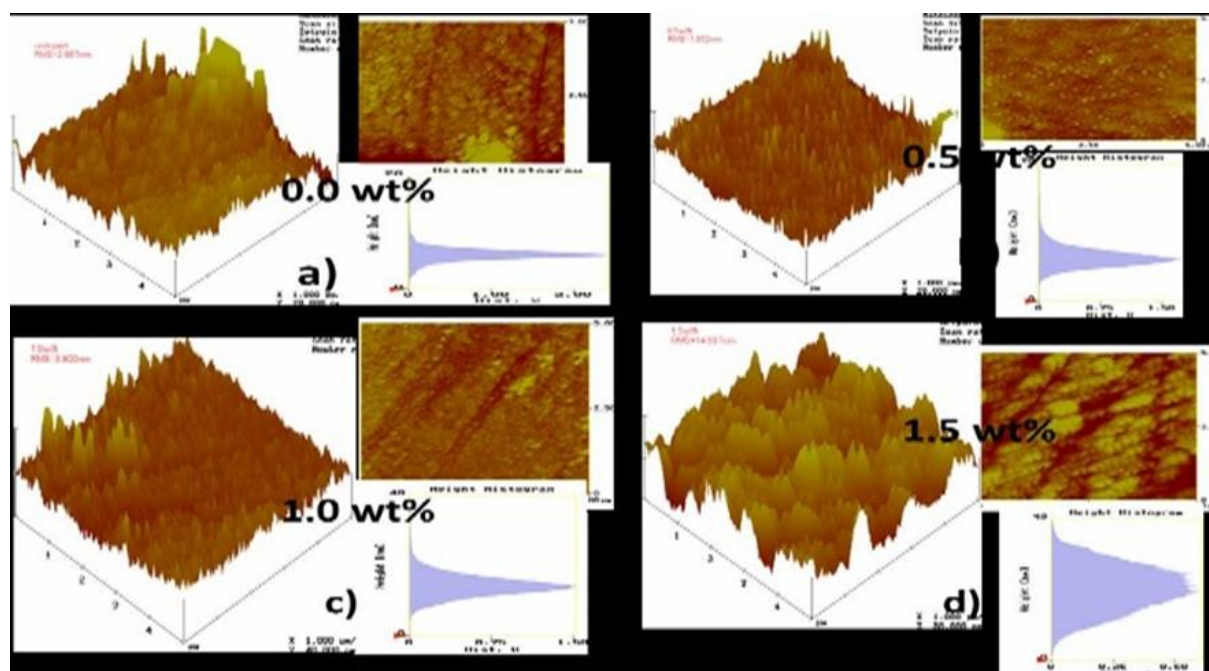


Figure 5: AFM Image of ZnO:Sc (Sc 0.0 to 1.5 wt. %) thin films annealed at 400 °C in nitrogen ambient atmosphere for 1 h.

Figure 5 manifest the AFM 3D and 2D images of thin ZnO:Sc films (0.0 to 1.5 wt%) annealed at 400 °C in a nitrogen ambient environment. Surface roughness falls significantly (from 28.8 nm to 4.7 nm) up to 0.5 wt% with an increase in Sc content. Particle sizes in ZnO:Sc (0.0 wt% to 1.5 wt%), films annealed in nitrogen ambient atmosphere were 124 to 160 nm while those in the films annealed under air ambient were 90-100 nm, respectively, analysed in AFM, Fig 5(a to d). AFM and SEM analysis of ZnO:Sc films revealed that the particle size is substantially greater than what XRD had indicated. This shows that whereas XRD provides the crystallite size, AFM provides the grain size (perhaps a few crystallites linked together).

Electrical properties

Figure 5 a–c delineates the effect of the annealing ambient environment on electrical characteristics (resistivity, carrier concentration, and Hall mobility) as a function of Scandium dopant concentration ZnO:Sc (0.0 wt% to 1.5 wt%). The annealing environment and temperature have an impact on the oxygen and zinc vacancies. Zinc vacancies get more activated when annealing atmosphere is rich in oxygen while the nitrogen atmosphere creates oxygen vacancies as well in addition to zinc vacancies. The oxygen vacancies are more pronounced at higher annealing temperatures and are characterized by higher concentrations of free charge carriers and mobility. As the optimized annealing temperature was 400°C, hence, the oxygen vacancies are likely to be formed more in nitrogen annealing atmosphere as compared to air annealed atmosphere, which is depicted in Fig 6a, 6b, and 6c. Whereas, the mobility and carrier concentration are higher while resistivity is lower for all the doped films annealed in the nitrogen atmosphere as to air atmosphere for ZnO:Sc [37-38].

Additionally, it is clear from Fig. 6c that as the Sc dopant concentration rises in both atmospheres from 0.0 wt% to 0.5 wt%, the resistivity dramatically drops. This inclination can

be elucidated by the fact that doping Sc³⁺ on the substitution site of Zn²⁺ ions and/or interstitial zinc atoms is restricted in both atmospheres when the carrier concentration increases (as shown in Fig. 6b) from 0.0 wt% to 0.5 wt%. It is remarkable that Hall mobility (μ_H) is maximum (40.28 cm²/Vs) and resistivity (ρ) is minimum (1.02 x 10⁻⁴ Ω -cm) in nitrogen annealing atmosphere as compared to the air annealing atmosphere ZnO:Sc (0.5 wt %). As shown in AFM and SEM images in Figures 3, 4, 5, and 6, as well as in published research [38], morphological changes with a denser structure, having fewer porosity/voids with a tight pack of nanograins connecting with one another in a nitrogen atmosphere support the aforementioned claim. The creation of more oxygen vacancies in the nitrogen environment contributing to n-type conductivity may be the other possibility. Oxygen and Nitrogen atoms having almost similar ionic radii but different chemical behavior favors Zn to make bonds with Oxygen atoms as compared to Nitrogen atoms resulting in low solubility for Nitrogen atoms. As a result, more oxygen vacancies are created and makes the Nitrogen atom as a shallow double donor [39].

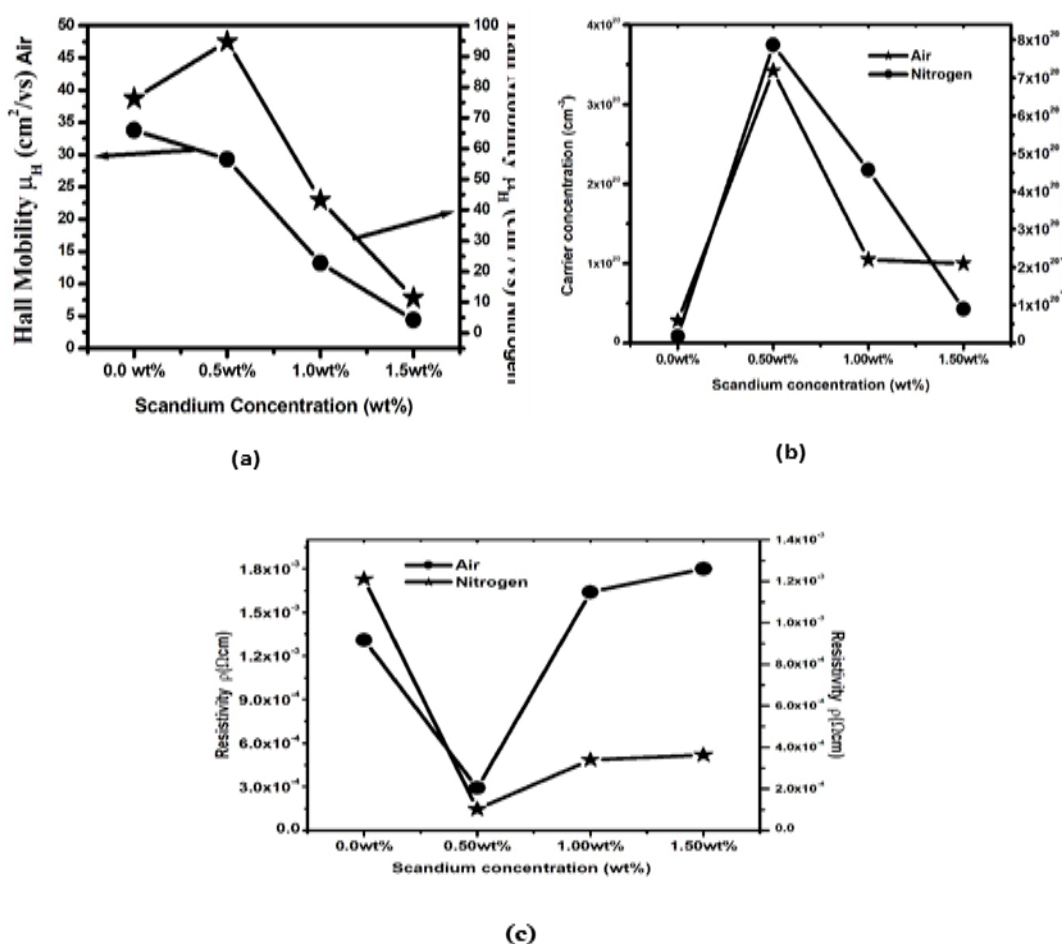


Figure 5: Change of (a) Resistivity (ρ), (b) Carrier concentration (n) and (c) Hall mobility (μ_H) as a function of Scandium dopant concentration (0.0 wt% to 1.5 wt%) annealed at 4000C temperatures in air and nitrogen ambient atmosphere respectively.

As the Sc dopant concentration in ZnO:Sc films increases from 0.0 wt % to 0.5 wt % carrier concentration increases from $4.8 \times 10^{19} \text{ cm}^{-3}$ to $5.47 \times 10^{20} \text{ cm}^{-3}$ and hall mobility increases from $71.65 \text{ cm}^2/\text{Vs}$ to $96.32 \text{ cm}^2/\text{Vs}$ films annealed in nitrogen atmosphere. The carrier concentration increases $3.2 \times 10^{19} \text{ cm}^{-3}$ to $3.27 \times 10^{20} \text{ cm}^{-3}$ and hall mobility decreases from $53.78 \text{ cm}^2/\text{Vs}$ to $40.28 \text{ cm}^2/\text{Vs}$ films annealed in air atmosphere for ZnO:Sc (1.0wt% to 1.5

wt%). As Sc concentration stimulation increases from 0.0 wt % to 0.5 wt % carrier concentration decline from $3.65 \times 10^{20} \text{ cm}^{-3}$ to $2.41 \times 10^{20} \text{ cm}^{-3}$ while hall mobility decreases $41.32 \text{ cm}^2/\text{Vs}$ to $12.74 \text{ cm}^2/\text{Vs}$ films annealed in nitrogen atmosphere. The carrier concentration decreases from $4.42 \times 10^{20} \text{ cm}^{-3}$ to $1.38 \times 10^{20} \text{ cm}^{-3}$ and hall mobility decreases from $13.22 \text{ cm}^2/\text{Vs}$ to $4.40 \text{ cm}^2/\text{Vs}$ films annealed in air atmosphere for ZnO:Sc (1.0wt% to 1.5 wt%). Due to the addition of more Sc ions ZnO:Sc (1.0wt% to 1.5 wt%), limited solubility, results in increasing defect scattering. Accessibility of oxygen in the grain boundaries guides to apprehend free electrons results in decrease in the concentration of free electrons as well as mobility. As Sc dopant concentrations increase carrier concentration of defects increases when annealed in the air atmosphere, resulting in more roughness as confirmed by SEM & AFM images, and hence, the resistivity increases. However, as seen in Fig. 6c, this increase in resistivity appears to be relatively minor in the nitrogen annealing atmosphere even though the carrier concentration falls as the Sc dopant concentration rises. This may be explained by the Fermi level shift in the conduction band observed in doped ZnO films that were annealed in nitrogen environment [40].

Optical properties

Transmittance:

Transmittance spectra in the 300–800 nm range were taken to investigate the effects of the annealing atmosphere (Air and Nitrogen) and the impact of Sc concentration ZnO:Sc (0.0 to 1.5 wt%) on optical properties. As shown in Fig. 6a, all deposited films exhibit increased optical transparency over the entire visible spectrum. The films' optical transmission spectrum shows an absorption edge at about 420 nm.

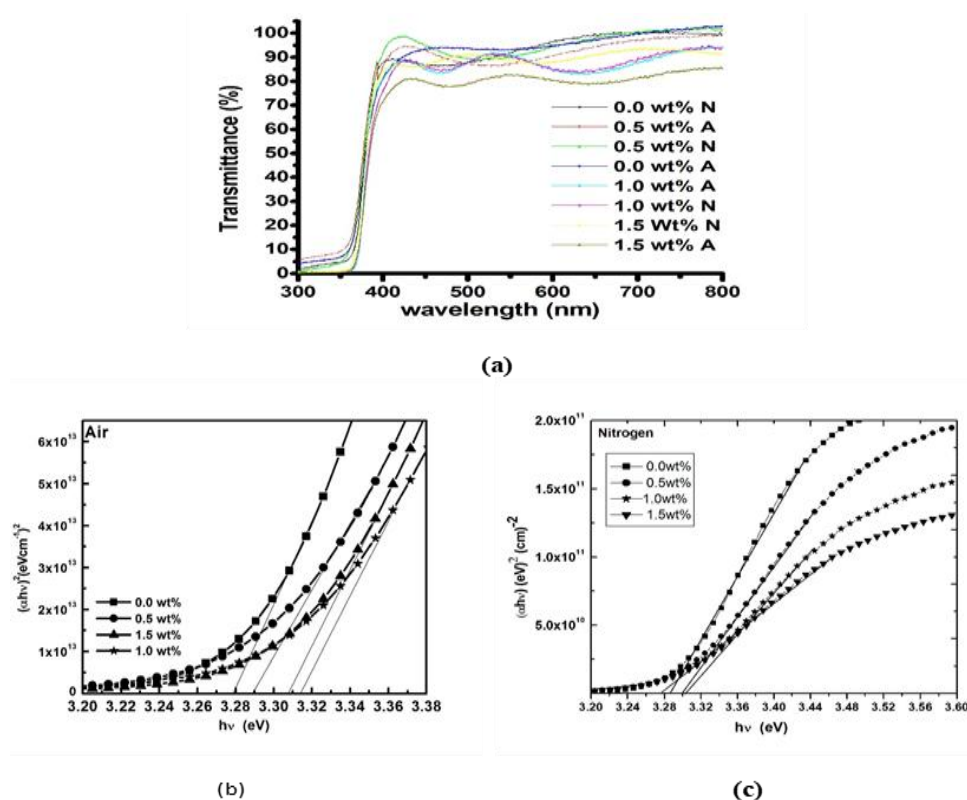


Figure 6: Variation of (a) Transmittance (T), (b & c) Bandgap E_g (eV) as a function of Scandium dopant concentration (0.0 wt% to 1.5 wt%) annealed at 400°C temperatures in air and nitrogen ambient atmosphere respectively.

According to the figure's transmission spectra, the average transmittance in the nitrogen atmosphere and the air atmosphere, respectively, is not less than 92% and 80%. The ZnO:Sc (0.0 to 1.5 wt%) films annealed in a nitrogen ambient atmosphere are more transparent than the films annealed in air ambient atmosphere. That could be elucidated as the covered grains in the nitrogen annealed atmosphere films are larger reducing inter-grain shadowing, and denser as comparison to the films annealed in the air ambient atmosphere. The XRD data and the SEM in Fig. 1 and 2, and AFM Fig.3 and 4 images [24] also confirm this. Maximum transmittance is observed for 0.0 wt % Sc doping ZnO:Sc films ~ 88% and decreases with the increase in ZnO:Sc (0.0 wt% to 1.5 wt%) concentration in the air ambient annealed films. This has a connection to the light loss brought on by doping's increased scattering centres. While, in nitrogen ambient annealed films, the transmittance detected is slightly complex.

It is observed that transmittance got increased in 0.5 wt % Sc doped in ZnO:Sc films as compared to other nitrogen ambient annealed films. The crystallinity of the films can be linked to this pattern. From XRD data (Fig. 1f) and SEM images (Fig. 2), it appears that the grain size and film quality in ZnO:Sc films improve with increasing Sc concentration (0.0 wt% to 0.5 wt%), which leads in an escalate in transmittance. The quality of ZnO:Sc films degrades when the concentration of Sc doping is increased (from 0.0 wt% to 1.5 wt%), as transmittance drops with it. ZnO: Sc(0.5 wt%) annealed in the nitrogen annealing atmosphere has the highest transmittance, which is 92%.

Bandgap:

For photon energy $h\nu$ enormous than the semiconductor's band gap energy E_g , the optical absorption coefficient of a direct band gap semiconductor near the band edge is given by [41].

$$\alpha h\nu = A (h\nu - E_g)^{1/2}$$

where α is optical absorption coefficient, A is constant, and ν is the frequency of the incident photon and h is Planck's constant. The transmission spectra will provide the value of α . In order to determine the band gap (Tauc's plot), the linear region of the plot of $(\alpha h\nu)^2$ as a function of the photo energy ($h\nu$) to the energy axis is extended as exhibited in Fig 6(b &c). When Sc doping is increased in ZnO:Sc (0.0 to 1.5wt%) films that have been annealed in air ambient environment atmosphere, it is discovered that the resultant band gap values are continually rising from 3.27 eV to 3.31 eV. The band gap values in the nitrogen-annealed ambient environment are in the 3.29–3.32 eV range.

The result specifies that the band gap increases slightly in the nitrogen annealed atmosphere as compared to the air annealed atmosphere. This increase might be perceived by the rise in the carrier concentration called the Burstein-Moss effect [42] as also evident from Fig 5b.

Reflection High Energy Electron Diffraction

From the above results, the films ZnO:Sc (0.5 wt%) show the best crystalline structure. The morphology indicates the existence of the uniformly distributed nano-rod-like structures with high compactness in the air annealed atmosphere Fig 2(b) and Fig 4(b), and the closely spaced polyhedral-shaped sintered grains with clear grain boundaries in the nitrogen annealed atmosphere Fig 3(b) and Fig 5(b). To look closer at the surface of these two cases, RHEED patterns were observed as it is an effective method for examining surface structure and organising phenomena. In Fig. 8(a), it is possible to discern a distinct set of concentric Debye rings, which point to the development of polycrystalline nanorods with numerous crystallites and random orientations in the air atmosphere. As long as there are no arcs in the rings, there

is no texture or preferred crystallite alignment in the grown film, which is evident from the continuous rings. A smooth single-crystal surface is indicated by streak-like patterns in the RHEED pattern of the 0.5 wt% Sc doped film that was annealed in the nitrogen atmosphere, as shown in Fig. 7(b) [43].

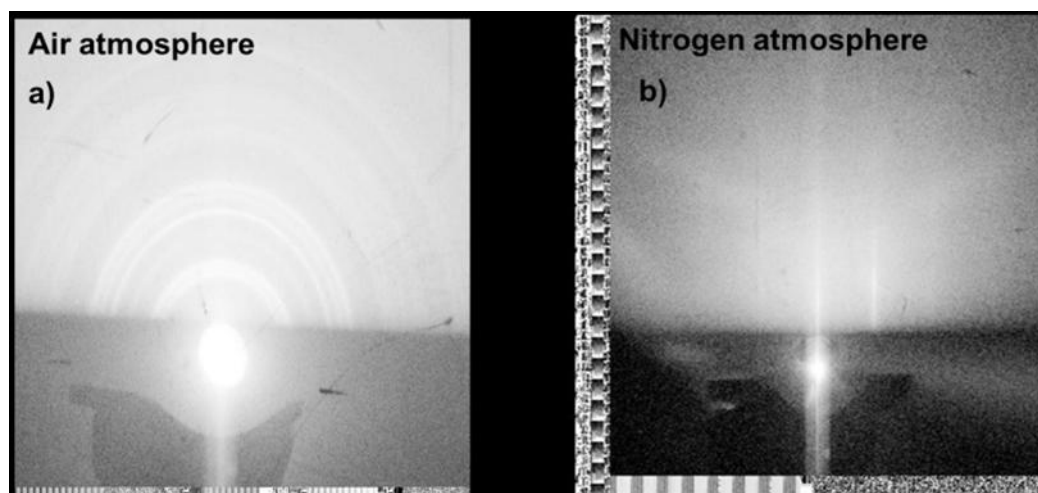


Figure 7: RHEED pattern of ZnO:Sc (0.5 wt%) films annealed at 4000C temperatures in a) air and b) nitrogen ambient atmosphere respectively.

From the above results, the films ZnO:Sc (0.5 wt%) show the best crystalline structure. The morphology indicates the existence of the uniformly distributed nano-rod-like structures with high compactness in the air annealed atmosphere Fig 1(b) and Fig 3(b), and the closely spaced polyhedral-shaped sintered grains with clear grain boundaries in the nitrogen annealed atmosphere Fig 2(b) and Fig 4(b). To look closer at the surface of these two cases, RHEED patterns were observed as it is an effective method for examining surface structure and organising phenomena. In Fig. 7(a), it is possible to discern a distinct set of concentric Debye rings, which point to the development of polycrystalline nanorods with numerous crystallites and random orientations in the air atmosphere. As long as there are no arcs in the rings, there is no texture or preferred crystallite alignment in the grown film, which is evident from the continuous rings. A smooth single-crystal surface is indicated by streak-like patterns in the RHEED pattern of the 0.5 wt% Sc doped film that was annealed in the nitrogen atmosphere, as shown in Fig. 7(b) [43].

CONCLUSION

Sol-gel spin coating routine was used to flourish Sc-doped ZnO:Sc (0.0 - 1.5 wt%) thin films onto corning glass (7059) substrates and annealed at 400 °C for 1 hour in nitrogen and air environments. The ZnO hexagonal wurtzite polycrystalline structure is evident in the crystal structure free of any impurity phases. It was discovered that the ZnO:Sc film's crystallinity and the preferred growth direction were significantly connected with the concentration of the dopant as well as different annealing ambient atmospheres. At the doping level of 0.5 wt%, the crystallinity of the films showed a remarkable improvement, but as doping continued, the crystallinity began to deteriorate. The film that was annealed in nitrogen achieved the greatest improvements in structural and electrical properties. The best crystalline film is obtained for ZnO:Sc (0.5 wt%) in both the atmosphere with the growth of polycrystalline nanorods in the air atmosphere and single crystals in the nitrogen atmosphere. The highest carrier concentration

and lowest resistivity are obtained for the ZnO:Sc (0.5 wt%) film annealed in the nitrogen atmosphere. In contrast to films that are annealed in air the films that are annealed in a nitrogen exhibit improved transmittance with a wider band gap. These high-quality conducting ZnO:Sc films on glass substrate, demonstrate the viability of using these films for optoelectronic device, LEDs, transistors, sensors, photodetectors and also as a conductive layer in solar cells on large-area substrates at a low cost.

ACKNOWLEDGEMENTS

Ruchika (Sharma) Joshi, one of the writers, expresses gratitude for the financial assistance provided by the Department of Physics, Deshbandhu College under the auspices of the IQAC and DBT STAR College Scheme. The authors also want to thank AIEJ, Japan, for providing financial support for the stay in Toyohashi University of Technology, Toyohashi, Japan.

REFERENCES

- [1] Michał A. Borysiewicz, ZnO as a Functional Material, a Review, Crystals, 9 (2019) 505, <https://doi.org/10.3390/cryst9100505>.
- [2] Young-Jin Kim and Hyeong-Joon Kim, Trapped oxygen in the grain boundaries of ZnO polycrystalline thin films prepared by plasma-enhanced chemical vapor deposition, Materials Letters, 41 (1999) 159-163, [https://doi.org/10.1016/S0167-577X\(99\)00124-X](https://doi.org/10.1016/S0167-577X(99)00124-X).
- [3] D. R. Lide, Hand Book of Chemistry and Physics, 71st ed. (CRC, Boca Raton, FL, 1991).
- [4] A. Ohtomo, M. Kawasaki, I. Ohkubo, H. Koinuma, T. Yasuda and Y. Segawa, Structure and optical properties of ZnO/Mg_{0.2}Zn_{0.8}O superlattices, Appl. Phys. Lett., 75 (1999) 980-982, <https://doi.org/10.1063/1.124573>.
- [5] Z. K. Tang, G. K. L. Wong, P. Yu, M. Kawasaki, A. Ohtomo, H. Koinuma and Y. Segawa, Room-Temperature Ultraviolet Laser Emission from Self-Assembled ZnO Microcrystallite Thin Films, Appl. Phys. Lett., 72 (1998) 3270-3272, [10.1063/1.121620](https://doi.org/10.1063/1.121620).
- [6] Studenikin A. S.; Golego Nickolay; Cocivera Michael, Optical and electrical properties of undoped ZnO films grown by spray pyrolysis of zinc nitrate solution, Journal of Applied Physics, 83 (1998), 2104-2111, [10.1063/1.366944](https://doi.org/10.1063/1.366944).
- [7] Zhengwei Li and Wei Gao, ZnO thin films with DC and RF reactive sputtering, Materials Letters, 58 (2004) 1363-1370, <https://doi.org/10.1016/j.matlet.2003.09.028>.
- [8] Song Dengyuan, Effects of rf power on surface-morphological, structural and electrical properties of aluminum doped zinc oxide films by magnetron sputtering, Applied Surface Science, 254 (2008) 4171-4178, <https://doi.org/10.1016/j.apsusc.2007.12.061>.
- [9] Fouad A. O.; Ismail A. A.; Zaki I. Z.; Mohamed M. R., Zinc oxide thin films prepared by thermal evaporation deposition and its photocatalytic activity. Applied Catalysis B: Environmental, 62 (2006) 144–149, <http://dx.doi.org/10.1016%2Fj.apcatb.2005.07.006>
- [10] Saito Koki; Watanabe Yuki; Takahashi Kiyoshi; Matsuzawa Takeo; Sang Baosheng; Konagai Makoto, Photo atomic layer deposition of transparent conductive ZnO films. Solar Energy Materials and Solar Cells, 49 (1997) 187-193, [https://doi.org/10.1016/S0927-0248\(97\)00194-3](https://doi.org/10.1016/S0927-0248(97)00194-3).
- [11] Natsume Y.; Sakata H.; Hirayama T., Low-Temperature electrical conductivity and optical absorption edge of ZnO films prepared by chemical vapor deposition, Phys. Stat. Sol. (a), 148 (1995) 485-495, <https://doi.org/10.1002/pssa.2211480217>.
- [12] Musat V.; Rego M. A.; Monteiro R.; Fortunato E., Microstructure and gas-sensing properties of sol-gel ZnO thin films, Thin Solid Films, 516 (2008) 1512-1515, <http://dx.doi.org/10.1016/j.tsf.2007.07.198>.
- [13] Singh V. A.; Mehra M. R.; Yoshida A.; Wakahara A., Doping mechanism in aluminium doped zinc oxide films, Journal of Applied Physics, 95 (2004), 3640-3643, <http://dx.doi.org/10.1063/1.1667259>.
- [14] LUlrike Heitmann, Johan Westraadt, Jacques O'Connell, Leonie Jakob, Frank Dimroth, Jonas Bartsch, Stefan Janz, and Jan Neethling, Spray Pyrolysis of ZnO:In: Characterization of Growth Mechanism and

- Interface Analysis on p-Type GaAs and n-Type Si Semiconductor Materials, ACS Appl. Mater. Interfaces, 14 (2022), 41149–41155, <https://doi.org/10.1021/acsami.2c07585>.
- [15] Studenikin A. S.; Golego Nickolay; Cocivera Michael, Fabrication of green and orange photoluminescent, undoped ZnO films using spray pyrolysis, Journal of Applied physics, 84 (1998) 2287-2294, <https://doi.org/10.1063/1.368295>.
- [16] Studenikin A. S.; Golego Nickolay; Cocivera Michael, Carrier mobility and density contributions to photoconductivity transients in polycrystalline ZnO films, Journal of Applied physics, 87 (2000) 2413-2421, <https://doi.org/10.1063/1.372194>.
- [17] Ikhmayies J. Shadia, Production and characterization of CdS/CdTe thin film photovoltaic solar cells of potential industrial use. Ph.D Thesis (2002), University of Jordan, Jordan, <https://doi.org/10.3929/ethz-a-004282736>.
- [18] Y. Takahashi, Y. Matsuoka, Dip-coating of TiO₂ films using a sol derived from Ti(O-i-Pr)₄-diethanolamine-H₂O-i-PrOH system, J. Mat. Sci., 23 (1988) 2259-2266, <https://doi.org/10.1007/BF01115798>
- [19] Y. Ohya, H. Saiki, Y. Takahashi, Preparation of transparent, electrically conducting ZnO film from zinc acetate and alkoxide, J. Mat. Sci., 29 (1994) 4099-4103, <https://doi.org/10.1007/BF00355977>
- [20] Y. Takahashi, S. Okada, R. B. H.Tahar, K. Nakano, T. Ban, Y. Ohya, Dip-coating of ITO films, J. Non.Cryst. Solids, 218 (1997) 129 -134, [https://doi.org/10.1016/S0022-3093\(97\)00199-3](https://doi.org/10.1016/S0022-3093(97)00199-3)
- [21] T. Tsuchiya, T. Emoto, T. Sei, Preparation and properties of transparent conductive thin films by the sol-gel process, J. Non. Cryst. Solids, 178 (1994) 327-332, [https://doi.org/10.1016/0022-3093\(94\)90302-6](https://doi.org/10.1016/0022-3093(94)90302-6)
- [22] A. Biswas, G. S. Maciel, C. S. Friend, P. N. Prasad, Upconversion properties of a transparent Er³⁺-Yb³⁺-co-doped LaF₃-SiO₂ glass-ceramics prepared by sol-gel method, J. Non. Cryst. Solids, 316 (2003) 393-397, [https://doi.org/10.1016/S0022-3093\(02\)01951-8](https://doi.org/10.1016/S0022-3093(02)01951-8).
- [23] T. Minami, T. Yamamoto, T. Miyata, Highly transparent and conductive rare earth-doped ZnO thin films prepared by magnetron sputtering, Thin Solid Films, 366 (2000) 63-68, [https://doi.org/10.1016/S0040-6090\(00\)00731-8](https://doi.org/10.1016/S0040-6090(00)00731-8).
- [24] R. Sharma, P.K. Shishodia, A. Wakahara, R.M. Mehra, Investigations of highly conducting and transparent Sc doped ZnO films grown by the sol-gel process, Mater. Sci.-Poland 27 (2009) 233–245
- [25] R. Kaur, A.V.Singh, R.M. Mehra, Sol-gel derived yttrium doped ZnO nanostructures, Journal of Non-Crystalline Solids, 352 (2006) 2565-2568, <https://doi.org/10.1016/j.jnoncrysol.2006.01.090>.
- [26] R. Sharma, A. Wakahara, R.M. Mehra, Epitaxial growth of highly transparent and conducting Sc-doped ZnO films on c-plane sapphire by sol-gel process without buffer, Current Applied Physics, 10 (2010) 164–170, <https://doi.org/10.1016/j.cap.2009.05.013>.
- [27] Michael Lorenz, Christian Schmidt, Gabriele Benndorf, Tammo Bontgen, Holger Hochmuth, Rolf Bottcher, Andreas Poppl, Daniel Spemann and Marios Grundmann, Degenerate interface layers in epitaxial scandium-doped ZnO thin films, J. Phys. D: Appl. Phys. 46 (2013) 065311, <http://dx.doi.org/10.1088/0022-3727/46/6/065311>
- [28] G. Newman, On the Defect Structure of Zinc-Doped Zinc Oxide, phys. stat. sol. b, 105 (1981) 605-612, <http://dx.doi.org/10.1002/pssb.2221050220>
- [29] Y. J. Kim, H. J. Kim, Trapped oxygen in the grain boundaries of ZnO polycrystalline thin films prepared by plasma-enhanced chemical vapor deposition, Material Letters, 41 (1999) 159-163, <https://portal.issn.org/resource/ISSN/0167-577X>
- [30] B.D. Cullity, Elements of X-ray Diffractions, Addison-Wesley, Reading, MA, 1978, ISBN 0-201-01174-3.
- [31] Miao Cun-Xing, Zhao Zhan-Xia, Zhao Lei and Ma Zhong-Quan, Substrate temperature dependence of the properties of scandium-doped ZnO films deposited by sputtering, Applied Surface Science, 256 (2010) 3174-3177, <https://doi.org/10.1016/j.apsusc.2009.12.001>
- [32] H. Akazawa, Substrate-dependent luminescent properties of thin-film phosphors: Comparative study of Eu³⁺-doped ZnO films deposited on SiO₂, Si, and sapphire substrates, Thin Solid Films., 689 (2019) 137513, <https://doi.org/10.1016/j.tsf.2019.137513>

- [33] M. A. M. Ahmed, W. E. Meyer, and J. M. Nel, Effect of (Ce, Al) co-doped ZnO thin films on the Schottky diode properties fabricated using the sol-gel spin coating, *Mater. Sci. Semicond. Process.*, 103 (2019) 104612, <https://doi.org/10.1016/j.mssp.2019.104612>
- [34] M. R. Islam, M. Rahman, S. F. U. Farhad, and J. Podder, Structural, optical and photocatalysis properties of sol-gel deposited Al-doped ZnO thin films, *Surfaces and Interfaces.*, 16 (2019) 120-126, <https://doi.org/10.1016/j.surfin.2019.05.007>
- [35] P. Hosseini Vajargah, H. Abdizadeh, R. Ebrahimifard, and M. R. Golobostanfard, Sol-gel derived ZnO thin films: Effect of amino-additives, *Appl. Surf. Sci.*, 285 (2013) 732-743, <http://dx.doi.org/10.1016/j.apsusc.2013.08.118>
- [36] R. Hayami, N. Endo, T. Abe, Y. Miyase, T. Sagawa, K. Yamamoto, S. Tsukada, and T. Gunji, Zinc-diethanolamine complex: Synthesis, characterization, and formation mechanism of zinc oxide via thermal decomposition, *J. Sol-Gel Sci. Techn.*, 87 (2018) 743-748, <https://doi.org/10.1007/s10971-018-4768-x>
- [37] Vitaly Gurylev, Tsong Pyng Perng, Defect engineering of ZnO: Review on oxygen and zinc vacancies, *Journal of the European Ceramic Society* 41 (2021) 4977–4996, <http://dx.doi.org/10.1016/j.jeurceramsoc.2021.03.031>
- [38] Wuttichai Sinornate, Hidenori Mimura and Wisanu Pecharapa Structural, Morphological, Optical and Electrical Properties of Sol-gel Derived Sb-doped ZnO Thin Films Annealed under Different Atmospheres, *Phys. Stat. Soli. A*, 28 (2020) 2000233, <https://doi.org/10.1002/pssa.202000233>
- [39] Yao S L, Hong J D, Lee C T, Ho C Y and Liu D S, Determination of activation behavior in annealed Al-N codoped ZnO Films, *J. Appl. Phys.*, 109 (2011) 103504, <https://doi.org/10.1063/1.3587164>
- [40] A. Ievtushenko, O. Khyzhun, I. Shteplyuk, O. Bykov, R. Jakiela, S. Tkach, E. Kuzmenko, V. Baturin, O. Karpenko, O. Olifan, G. Lashkarev, X-ray photoelectron spectroscopy study of highly-doped ZnO:Al,N films grown at O-rich conditions, *Journal of Alloys and Compounds*, 722 (2017) 683-689, <http://dx.doi.org/10.1016/j.jallcom.2017.06.169>
- [41] Szczyrbowski J., Dietrich A., Hoffmann H., Optical and electrical properties of RF-sputtered indium-tin oxide films, *Phys. Stat. Sol. a*, 78 (1983), 243-252, <https://doi.org/10.1002/pssa.2210780129>
- [42] MOSS T.S., The Interpretation of the Properties of Indium Antimonide, *Proc. Phy. Soc. B*, 67 (1954) 775, https://ui.adsabs.harvard.edu/link_gateway/1954PPSB...67.775M/doi:10.1088/0370-1301/67/10/306
- [43] F Tang, T Parker, G-C Wang and T-M Lu, Surface texture evolution of polycrystalline and nanostructured films: RHEED surface pole figure analysis, *J. Phys. D: Appl. Phys.*, 40 (2007) R427, <http://dx.doi.org/10.1088/0022-3727/40/23/R01>.



This is an open access article distributed under the terms of the Creative Commons NC-SA 4.0 License Attribution—unrestricted use, sharing, adaptation, distribution and reproduction in any medium or format, for any purpose non-commercially. This allows others to remix, tweak, and build upon the work non-commercially, as long as the author is credited and the new creations are licensed under the identical terms. For any query contact: research@ciir.in